

8-2008

## Role Of Adenine In Thymine-dimer Repair By Reduced Flavin-adenine Dinucleotide

Guifeng Li

Vincent Sichula

Ksenija D. Glusac

*Bowling Green State University*, [kglusac@bgsu.edu](mailto:kglusac@bgsu.edu)

Follow this and additional works at: [https://scholarworks.bgsu.edu/chem\\_pub](https://scholarworks.bgsu.edu/chem_pub)

 Part of the [Chemistry Commons](#)

---

### Repository Citation

Li, Guifeng; Sichula, Vincent; and Glusac, Ksenija D., "Role Of Adenine In Thymine-dimer Repair By Reduced Flavin-adenine Dinucleotide" (2008). *Chemistry Faculty Publications*. 95.  
[https://scholarworks.bgsu.edu/chem\\_pub/95](https://scholarworks.bgsu.edu/chem_pub/95)

This Article is brought to you for free and open access by the Chemistry at ScholarWorks@BGSU. It has been accepted for inclusion in Chemistry Faculty Publications by an authorized administrator of ScholarWorks@BGSU.

# Role of Adenine in Thymine-Dimer Repair by Reduced Flavin-Adenine Dinucleotide

Guifeng Li, Vincent Sichula, and Ksenija D. Glusac\*

Department of Chemistry and Center for Photochemical Sciences, Bowling Green State University, Bowling Green, Ohio 43403

Received: May 21, 2008

We present a study of excited-state behavior of reduced flavin cofactors using femtosecond optical transient absorption spectroscopy. The reduced flavin cofactors studied were in two protonation states: flavin-adenine dinucleotide ( $\text{FADH}_2$  and  $\text{FADH}^-$ ) and flavin-mononucleotide ( $\text{FMNH}_2$  and  $\text{FMNH}^-$ ). We find that  $\text{FMNH}^-$  exhibits multiexponential decay dynamics due to the presence of two bent conformers of the isoalloxazine ring.  $\text{FMNH}_2$  exhibits an additional fast deactivation component that is assigned to an iminol tautomer. Reduced flavin cofactors also exhibit a long-lived component that is attributed to the semiquinone and the hydrated electron that are produced in photoinduced electron transfer to the solvent. The presence of adenine in  $\text{FADH}_2$  and  $\text{FADH}^-$  further changes the excited-state dynamics due to intramolecular electron transfer from the isoalloxazine to the adenine moiety of cofactors. This electron transfer is more pronounced in  $\text{FADH}_2$  due to  $\pi$ -stacking interactions between two moieties. We further studied cyclobutane thymine dimer (TT-dimer) repair via  $\text{FADH}^-$  and  $\text{FMNH}^-$  and found that the repair is much more efficient in the case of  $\text{FADH}^-$ . These results suggest that the adenine moiety plays a significant role in the TT-dimer repair dynamics. Two possible explanations for the adenine mediation are presented: (i) a two-step electron transfer process, with the initial electron transfer occurring from flavin to adenine moiety of  $\text{FADH}^-$ , followed by a second electron transfer from adenine to TT-dimer; (ii) the preconcentration of TT-dimer molecules around the flavin cofactor due to the hydrophobic nature of the adenine moiety.

## Introduction

Flavin cofactors are well-known electron-shuffle agents in biological systems due to their high reduction potentials and flexibility in mediating either one- or two-electron transfer processes. Apart from this “dark” role, flavoproteins are also known to perform light-driven catalysis. For example, phototropins<sup>1</sup> and BLUF proteins<sup>2</sup> regulate bending of plants and motion of microorganism toward light. In these proteins, the flavin cofactor is in its oxidized state. The reduced flavin cofactor is present in DNA photolyase<sup>3</sup> and cryptochrome<sup>4</sup> protein families. While the structures of these two classes of proteins are similar, their function in nature is different: photolyases repair cyclobutane thymidine-dimer lesions in DNA, while cryptochromes regulate the circadian rhythm.

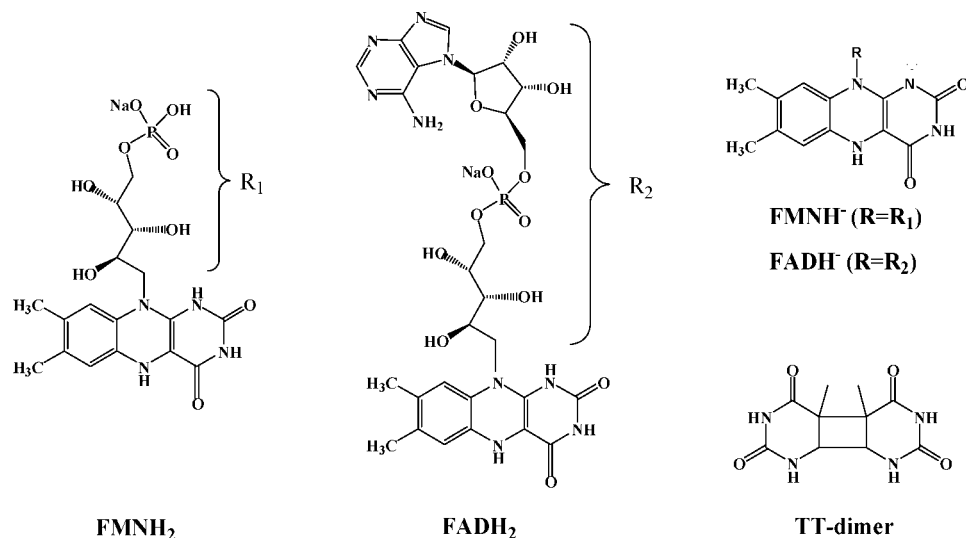
The mechanism of DNA repair by photolyase involves an electron transfer from photoexcited reduced and deprotonated flavin-adenine dinucleotide ( $\text{FADH}^-$ ) to the thymidine dimer (TT-dimer) lesion. The produced radical anion of TT-dimer undergoes a cycloreversion process within 560 ps<sup>5</sup> to produce thymidine and thymidine radical anion. The back electron transfer from the thymidine radical anion to the semiquinone recovers the flavin catalyst. While the mechanism of the process is known, it is still not clear what the factors are that contribute to the repair efficiency of almost unity.<sup>6</sup> One proposed explanation is a two-step electron transfer process, mediated by the adenine moiety of  $\text{FADH}^-$ .<sup>7</sup> This mechanism is supported by the fact that the photoinduced electron transfer from the excited flavin moiety of  $\text{FADH}^-$  to its adenine moiety is a thermodynamically favored process, with a driving force of  $\Delta G \sim -0.8$  eV. In addition, the conformation of the flavin cofactor in DNA photolyase supports the two-step electron transfer process. While

most of the flavoproteins exhibit their cofactors in an ‘open’ conformation with flavin and adenine moieties far away from each other, DNA photolyase is a rare example that has the cofactor in the U-shaped conformation with the two moieties in close proximity.<sup>8</sup> This unique cofactor conformation might have been chosen by nature to facilitate the electron transfer between the two moieties of  $\text{FADH}^-$ . However, no experimental verification has been presented that corroborates its existence.

In order to better understand the role of adenine in photocatalysis by flavins, we present a comparative study of excited-state dynamics of aqueous solutions of two reduced flavin cofactors: flavin-mononucleotide ( $\text{FMNH}_2$ ) and flavin-adenine dinucleotide ( $\text{FADH}_2$ ) presented in Scheme 1. The spectroscopy of flavins in their oxidized form has been extensively studied with both steady-state and time-resolved methods.<sup>9–14</sup> In addition, our group has recently reported a comprehensive pH-dependent study of FAD and FMN cofactors using femtosecond optical transient absorption spectroscopy.<sup>15</sup> On the other hand, reduced flavin cofactors have been studied much less<sup>16–25</sup> for several reasons: (i) low fluorescence quantum efficiency;<sup>17</sup> (ii) absorption bands are structureless in the UV/vis region;<sup>18</sup> (iii) due to the reactivity of reduced flavins with oxygen, the experiments must be conducted in an inert environment. The time-resolved fluorescence experiments of various reduced flavins were obtained by Visser and coauthors,<sup>17</sup> who found that the decays are usually described by at least three exponentials, suggesting that the excited-state dynamics of reduced flavins arise from several species. From NMR studies,<sup>21,23,24</sup> it is known that the central isoalloxazine ring of reduced flavins adopts a boat conformation and can undergo interconversion between one boat conformation to another. These NMR findings suggest that the complex excited-state dynamics of reduced flavins arise from contributions of different flavin conformers. In this work,

\* Corresponding author. E-mail: kglusac@bgsu.edu.

## SCHEME 1: Structures of Compounds Studied in This Work



we investigate the pH-dependent excited-state dynamics of  $\text{FMNH}_2$  and  $\text{FADH}_2$  using femtosecond optical transient absorption spectroscopy. We find that  $\text{FMNH}^-$  exhibits multi-exponential decay dynamics due to the presence of two boat conformers of the isoalloxazine ring.  $\text{FMNH}_2$  exhibits an additional fast excited-state deactivation, which we ascribe to the iminol tautomer of  $\text{FMNH}_2$ . In addition, both  $\text{FMNH}^-$  and  $\text{FMNH}_2$  contain a long-lived component that arises because of photoinduced electron transfer to solvent to produce a hydrated electron and a semiquinone radical. The presence of the adenine moiety in  $\text{FADH}_2$  influences the excited-state dynamics, by slowing down the “butterfly” motion and by inducing a photoinduced electron transfer process from the flavin to the adenine.

We further investigated the repair of TT-dimer using  $\text{FMNH}^-$  and  $\text{FADH}^-$  and found that the repair dynamics are faster in  $\text{FADH}^-$ . These results are discussed in terms of a two-step electron transfer model and the preconcentration of TT-dimer around  $\text{FADH}^-$ .

### Experimental Section

**Sample Preparation.** Flavin adenine dinucleotide disodium salt hydrate (FAD, HPLC grade) was purchased from Sigma, while flavin mononucleotide monosodium salt dihydrate (FMN, practical grade) was purchased from MP Biomedicals. Sodium hydroxide (NaOH, 97.4%, EMD), potassium phosphate (monobasic,  $\text{KH}_2\text{PO}_4$ , 99%, Aldrich Chemical Co., Inc.), and phosphoric acid ( $\text{H}_3\text{PO}_4$ , 85%, Lehigh Valley Chemical) were used to prepare phosphate buffer solutions. All of these chemicals were used as received. Sodium dithionite was purchased from EMD ( $\text{Na}_2\text{S}_2\text{O}_4$ , 87%).

**$\text{FMNH}^-$  and  $\text{FADH}^-$  Samples.** FAD/FMN samples were dissolved in 11 mM phosphate buffer solutions with pH value from 3 to 11, respectively. The 11 mM phosphate buffers with different pH values were prepared as follows: first, 0.748 g  $\text{KH}_2\text{PO}_4$  was dissolved in 500 mL of deionized water, and then NaOH and  $\text{H}_3\text{PO}_4$  were used to exactly adjust different pH values. The solution pH values were measured with an Oakton pH meter (pHTestr Basic). After 20 mL of FAD/FMN buffer solution was purged for 15–20 min by argon, sodium dithionite (15 equivalents) was dissolved in about 0.2 mL of deionized water, and this solution was transferred into FAD/FMN buffer solution.<sup>26</sup> The solutions were placed in a quartz cell with 2

mm path length (Starna Cells, Inc.). The flavin concentrations were such that the absorption at 400 nm was in the 0.6–1.0 range. The absorption measurements were done using a UV–visible spectrophotometer (Varian Cary 50 Bio).

**TT-Dimer.** TT-dimer was synthesized according to the procedure by Wulff and Fraenkel.<sup>27</sup> Briefly, 0.250 g of thymine was dissolved in 250 mL of  $\text{H}_2\text{O}$ , and the solution was frozen at  $-80^\circ\text{C}$ . The frozen solution was transferred into a dry ice bath and irradiated by a UV lamp (PC451050, 450 W from Hanovia). The solution was then thawed, frozen again, and irradiated. The procedure was repeated four times. After irradiation, the solution was concentrated, filtered, and allowed to crystallize at  $5^\circ\text{C}$  overnight.

**Femtosecond Optical Transient Absorption Measurements.** The laser system for the ultrafast transient absorption measurement was described previously.<sup>28</sup> Briefly, the 800 nm laser pulses were produced at a 1 kHz repetition rate by a mode-locked Ti:Sapphire laser (Hurricane, Spectra-Physics). The pulse width was determined to be  $\text{fwhm} = 110$  fs using an autocorrelator (Positive Light). The output from the Hurricane was split into pump (85%) and probe (8%) beams. The pump beam (800 nm) was sent into a second harmonic generator (Super Tripler, CSK) to obtain a 400 nm excitation source. The energy of the pump beam was  $\sim 5$   $\mu\text{J}/\text{pulse}$ . The probe beam (800 nm) was delayed by a delay stage (MM 4000, Newport) and then focused into a Sapphire crystal for a white light continuum generation between 450 and 900 nm. An optical chopper was used to modulate the excitation beam at the 100 Hz frequency and to obtain the value of the transient absorption signal. The relative polarization between the pump and probe beams was set at the magic angle ( $54.7^\circ$ ). The pump and probe beams were overlapped in the sample. A smaller magnetic stirrer was put into a 0.7 mL rectangular quartz cell with 2 mm path length (Starna Cells, Inc.) to prevent sample photodegradation. After being passed through the cell, the continuum was coupled into an optical fiber and input into a CCD spectrograph (Ocean Optics, S2000). The data acquisition was achieved using in-house LabVIEW (National Instruments) software routines. The data were processed for chirp correction and noise reduction using the previously published procedure.<sup>15</sup> Briefly, the group velocity dispersion of the probing pulse was determined using nonresonant optical Kerr effect (OKE) measurements<sup>29</sup> on carbon

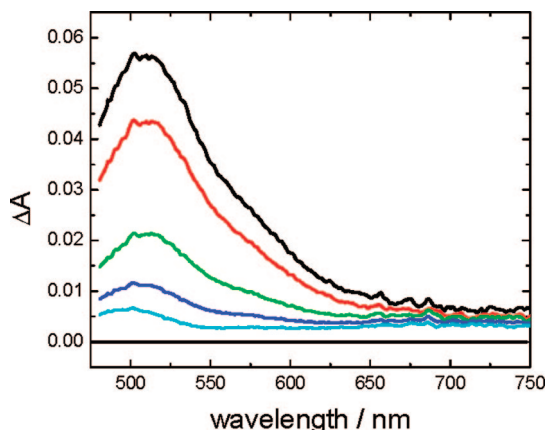


**Figure 1.** Transient absorption spectra of  $\text{FMNH}^-$  obtained at different probe delays: 1 ps (black); 10 ps (red); 50 ps (green); 100 ps (blue), 1200 ps (magenta).

tetrachloride solution. The noise in the data was reduced using a singular value decomposition (SVD) method (Matlab 7.1).

**Data Analysis.** Transient absorption data were analyzed using SPECFIT/32 Global Analysis System (Spectrum Software Associates). This program allows a decomposition of transient absorption data using kinetic models. The fitting process returns the predicted absorption spectra of individual colored species involved in the photochemical process along with their decay profiles. The analysis is achieved by a global analysis method that uses a singular value decomposition method to reduce the size of the fitted data.<sup>30</sup>

## Results and Discussion

**$\text{FMNH}_2$  and  $\text{FMNH}^-$ .** We will start our discussion with the dynamics of the reduced FMN cofactor. In this case, the excited-state behavior is governed only by the isoalloxazine moiety of the molecule. It represents the basis for our further investigations involving the role of adenine moiety in the dynamics of the reduced FAD.

We obtained transient absorption (TA) spectra of  $\text{FMNH}_2$  (pH = 5) and  $\text{FMNH}^-$  (pH = 11;  $\text{p}K_a$  value for  $\text{FMNH}_2$  is 6.7<sup>31</sup>). Qualitatively, the spectral characteristics of both species are similar. As an example, Figure 1 presents TA spectra for  $\text{FMNH}^-$  at different probe delays. The spectrum obtained 1 ps after the excitation pulse consists of an absorption band with a maximum at 507 nm that tails throughout the red portion of the visible spectrum. At subsequent time delays, the decay of this absorption band occurs, followed by an appearance of a new absorption band. The shape of the new absorption band can be best seen at time delay of 1200 ps. It consists of two absorption features: one centered at  $\sim 495$  nm and the other broadband centered at  $\sim 725$  nm.

The excited-state dynamics of  $\text{FMNH}^-$  are relatively complex: a three-exponential decay function is required to fit the data (Figure 2). The first two decays exhibit lifetimes of 40 and 530 ps, while the third component is long, it shows no observable decay during the time window of our measurement. Table 1 lists the lifetimes obtained by simultaneously fitting the decays at all wavelengths of the spectrum, while Figure 4 shows the absorption spectrum of each of the components obtained using Specfit software. Time-resolved fluorescence measurements on  $\text{FMNH}^-$  were done previously by Visser and coauthors.<sup>16,17</sup> Their results show that  $\text{FMNH}^-$  fluorescence consists of two components with lifetimes of 0.12 and 1.41 ns. The authors also observe a third long-lived component (5.27

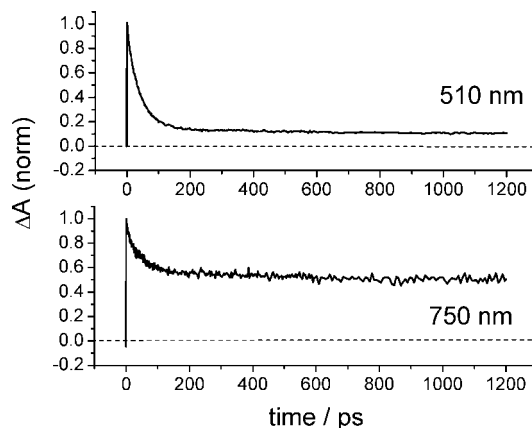


**Figure 2.** The transient absorption decays of  $\text{FMNH}^-$  solution collected at 510 and 750 nm.

**TABLE 1: Excited State Lifetimes of Different Flavin Cofactors<sup>a</sup>**

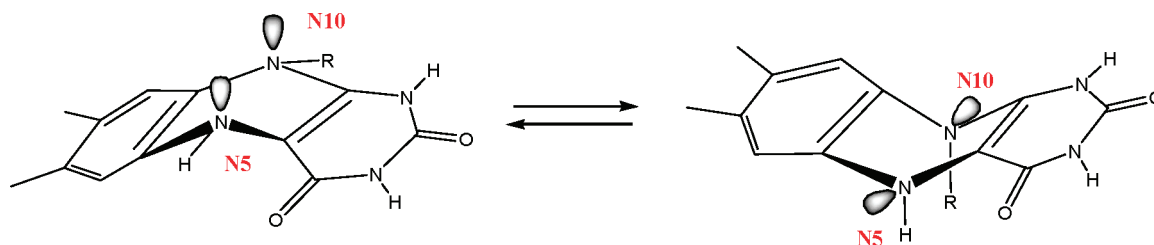
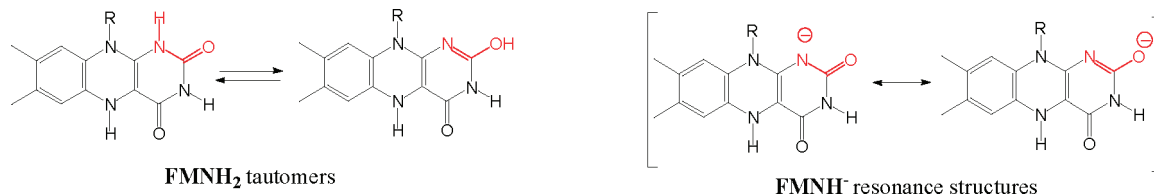
	$\tau_1$	$\tau_2$	$\tau_3$	$\tau_4$
$\text{FMNH}^-$	-	40 ps	529 ps	long
$\text{FADH}^-$	-	23 ps	401 ps	long
$\text{FMNH}_2$	3 ps	43 ps	793 ps	long
$\text{FADH}_2$	4 ps	53 ps	1.8 ns	long

<sup>a</sup> The measurements were performed in aqueous phosphate buffer solution.

ns) that has a very small contribution (less than 1%) to overall fluorescence. We do not observe this decay, probably because of the lower sensitivity of the TA technique. The two shorter-lived components observed by Visser are probably the same as the same as the ones that we observe in our measurements, except that our lifetimes are shorter than those reported by Visser. This discrepancy could be due to the fact that TA measurements require more concentrated solutions than fluorescence measurements. Thus, the shorter lifetime observed in our experiment could be due to increased rates of energy transfer between chromophores in the solution.

In agreement with the work done by Visser, we assign the two excited-state components to two distinct  $\text{FMNH}^-$  conformers. It is known from crystallography studies<sup>32</sup> that reduced flavins adopt a bent geometry, with the central ring of the isoalloxazine moiety in the boat conformation. NMR studies<sup>23</sup> show that reduced flavins undergo a fast conformational change from one boat conformer to another (“butterfly” motion, Scheme 2). The conformational change is too fast to be detectable on the NMR time scale (millisecond range) in the case of  $\text{FMNH}^-$ , but the process is detected if the flavin contains bulky substituents. It is known that the electronic properties of reduced flavins are very sensitive to conformational changes. This seems to be one of the main reasons why flavins are Nature’s choice for redox catalysis: different proteins can tune the standard reduction potentials of the same flavin cofactor from +80 to  $-500$  mV,<sup>33</sup> by forcing the reduced form into a specific conformation. Considering such large conformation-induced changes in the electronic properties of reduced flavins, it is not surprising that two boat conformers exhibit distinct optical properties, and that we observe two absorption bands in the TA spectra. It is not clear, however, whether the two conformers interconvert during their excited-state lifetime. The computational studies done by Hall suggest that the activation barrier for interconversion in the ground-state is 8.3 kJ/mol.<sup>34</sup> Assuming that the frequency factor is  $\sim 1 \times 10^{13} \text{ s}^{-1}$ , we use Arrhenius rate equation to estimate the rate of the conformational change to be  $3.5 \times 10^{11}$

## SCHEME 2: Structures of Two Boat Conformers Present in Reduced Flavin Solutions

SCHEME 3: The Structures of Tautomers Possibly Present in FMNH<sub>2</sub> Solution and Analogous Resonance Structures Present in FMNH<sup>-</sup>

s<sup>-1</sup> (half-time of 3 ps). Information on the activation barrier in the excited-state is not available, since the molecule is too large for reliable computational studies. However, if the activation barrier were similar to the one in the ground state, the conformational change could be occurring along the excited-state potential energy surface.

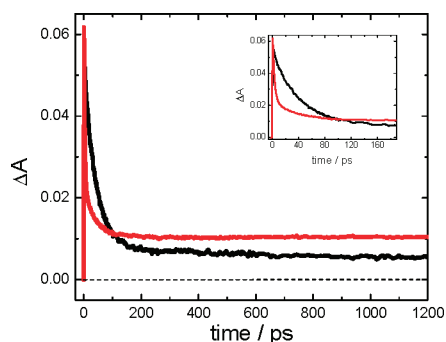
The dynamics of protonated FMNH<sub>2</sub> are different from FMNH<sup>-</sup> (Figure 3). Table 1 compares the lifetimes obtained by fitting FMNH<sup>-</sup> and FMNH<sub>2</sub> decays simultaneously at all wavelengths of the spectrum, while Figure 4 presents the absorption spectra of the species obtained by deconvolution of the TA data using Specfit software. As we can see, FMNH<sub>2</sub> contains the same components as FMNH<sup>-</sup>, but it also exhibits an additional short decay component with a lifetime of 3 ps. Since the only difference between the two species is the presence of an H-atom at N1-position in FMNH<sub>2</sub>, we initially assumed that the fast decay originates from the excited-state deprotonation of the N1 proton. The excited-state acidity of the molecule can be estimated from the pH-dependent ground-state absorption spectra using Forster cycle equation:<sup>35</sup>

$$pK_a - pK_a^* = \frac{h\nu_{\text{FIH}_2} - h\nu_{\text{FIH}^-}}{2.3RT} \quad (1)$$

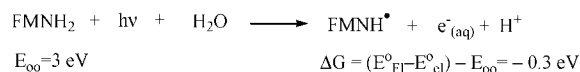
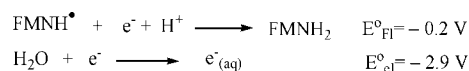
Here, pK<sub>a</sub> and pK<sub>a</sub><sup>\*</sup> are the ground and excited-state acidity of the reduced flavin, while hν<sub>FIH<sub>2</sub></sub> and hν<sub>FIH<sup>-</sup></sub> are the absorption energies of the protonated and deprotonated flavin. Using the value of pK<sub>a</sub> = 6.7<sup>31</sup> and the absorption spectra obtained in ref 20, we estimate the excited-state acidity constant of flavin to be 1.08 pH units larger than the ground-state acidity (pK<sub>a</sub><sup>\*</sup> ~

7.78). Thus, the short-lived component observed at pH = 5 probably does not arise from the excited-state deprotonation. An alternative explanation for the short-lived component is the presence of two tautomers in FMNH<sub>2</sub>. We propose that a certain amount of FMNH<sub>2</sub> is present in the form of an iminol tautomer that gives rise to a short-lived component (Scheme 3). In the basic region, we do not observe these tautomers because the delocalization of the negative charge in FMNH<sup>-</sup> gives rise to indistinguishable resonance structures.

So far we discussed the possible assignments of the short-lived components in the excited-state decay of FMNH<sub>2</sub>. The long-lived component observed in the TA spectra of FMNH<sup>-</sup> and FMNH<sub>2</sub> still remains unaccounted for. The red lines in the lower panels of Figure 4 (τ<sub>4</sub> components) present the spectrum of this long-lived component, which consists of two absorption bands: one with the maximum at ~500 nm and another broadband with the maximum ~725 nm. These features are similar to the spectra obtained by Heelis and coauthors using nanosecond laser flash photolysis.<sup>25</sup> The authors find that the 725 nm component disappears in the presence of N<sub>2</sub>O and thus assign it to the hydrated electron. It is known that the hydrated electron exhibits a broad absorption band with a maximum at 720 nm.<sup>36</sup> The 500 nm component was then assigned to the flavin semiquinone absorption. The neutral semiquinone has a broad absorption with maxima at 495 and 600 nm.<sup>37</sup> Thus, it is quite possible that the long-lived component arises from the photoinduced electron transfer to produce hydrated electron is a spontaneous process (Scheme 4). In addition, the reduced FMNH<sub>2</sub> has been previously shown to catalyze the photoinduced hydrogen production.<sup>38</sup> The hydrated electron is probably the

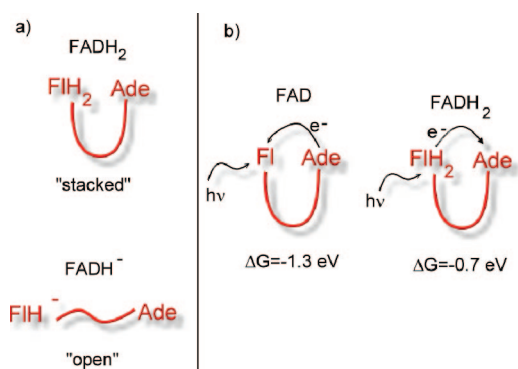


**Figure 3.** Transient absorption decays of FMNH<sup>-</sup> (black) and FMNH<sub>2</sub> (red) obtained at 510 nm.

SCHEME 4: Calculation of the Driving Force (ΔG) for Photoinduced Electron Transfer from Excited FMNH<sub>2</sub> to Water<sup>a</sup>

<sup>a</sup> The standard reduction potential for FMNH<sub>2</sub> was obtained from ref 33 while the one electron reduction potential of water was obtained from ref 42.

**SCHEME 5: (a) Schematic Representations of Stacked Conformer Present in FADH<sub>2</sub> and Open Conformer Present in FADH<sup>-</sup>; (b) Intramolecular Photoinduced Electron Transfer in FAD and FADH<sub>2</sub>**



initial product of this process that further reacts with H<sup>+</sup> ions to produce hydrogen atoms, which finally unite into molecular hydrogen. We believe that the longer-lived conformers of FMNH<sup>-</sup> ( $\tau = 529$  ps) and FMNH<sub>2</sub> ( $\tau = 793$  ps) deactivate by a photoinduced electron transfer process to produce hydrated electron and a semiquinone. As expected, deactivation is faster for FMNH<sup>-</sup>, which is consistent with the fact that FMNH<sup>-</sup> is a stronger reducing agent than FMNH<sub>2</sub>.

**FADH<sub>2</sub> and FADH<sup>-</sup>.** Adenine-containing flavin cofactors in the oxidized state are known to exhibit additional complexity due to  $\pi$ -stacking interactions between isoalloxazine and adenine moieties.<sup>9,11–15</sup> Specifically, aqueous solution of FAD contains two conformers: an "open" conformer in which isoalloxazine and adenine rings are far away from each other, and a "stacked" conformer in which the two moieties form a  $\pi$ -complex. The amount of "open" conformer increases as one of the moieties develops charge. For example, in a neutral solution most of FAD exists in a "stacked" conformation, while protonation of the adenine moiety at pH < 3 or deprotonation of the isoalloxazine ring at pH > 10 leads to breakage of the  $\pi$ -complex and a preferential formation of an "open" conformer. In analogy to the oxidized FAD, we expect FADH<sub>2</sub> to show the same behavior: at pH = 5, the "stacked" conformer should be dominant, while at pH = 11, the open conformer should exist (Scheme 5a). The  $\pi$ -complex formed in FADH<sub>2</sub> is expected to be weaker than in FAD, because the isoalloxazine ring is planar in oxidized FAD, whereas it is bent in reduced FADH<sub>2</sub>. In a "stacked" FAD conformer, the excited-state lifetime is significantly shorter than in an "open" form, possibly due to photoinduced electron transfer from adenine to the excited isoalloxazine ( $\Delta G \sim -1.3$  eV<sup>15</sup>). In "stacked" FADH<sub>2</sub>, the electron transfer could occur in the opposite direction, from isoalloxazine to adenine. Using a flavin standard reduction potential of  $E = -0.2$  V,<sup>33</sup> an adenine standard reduction potential of  $E = -2.5$  V<sup>39</sup> and an energy of the absorbed photon  $E_{00} = 3$  eV, we estimate the driving force for the electron transfer to be  $\Delta G \sim -0.7$  eV (Scheme 5b).

With this knowledge, we turn our attention to the results obtained from transient absorption measurements of FADH<sup>-</sup> and FADH<sub>2</sub>. The lower panel of Figure 5 compares the decays of FMNH<sup>-</sup> and FADH<sup>-</sup> obtained at 500 nm. Similarly to FMNH<sup>-</sup>, the decay dynamics of FADH<sup>-</sup> fit to a three-exponential decay function. However, the FADH<sup>-</sup> lifetimes are somewhat shorter, as shown in Table 1. In addition, we compared the absorption spectra of each of the decay components in FADH<sup>-</sup> to those obtained for FMNH<sup>-</sup> (Figure 4). The results show that the absorbing species in FADH<sup>-</sup> and FMNH<sup>-</sup>

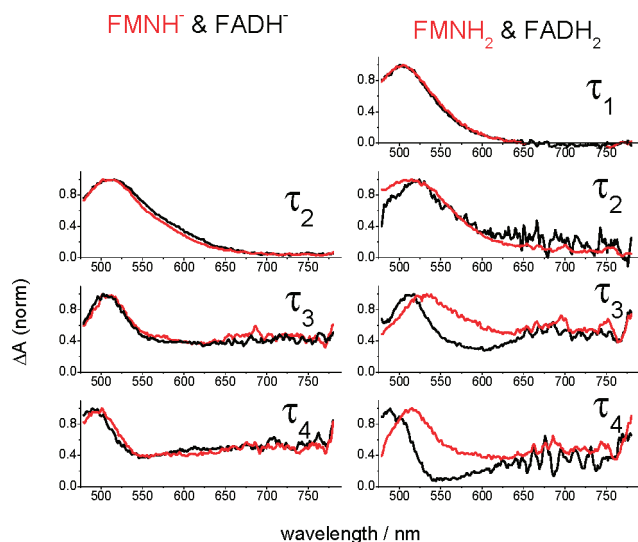


**Figure 4.** Spectra of different species involved in excited-state dynamics of flavin cofactors. Left panels: data obtained at pH = 11 (FMNH<sup>-</sup>: red curves; FADH<sup>-</sup>: black curves). Right panels: data obtained at pH = 5 (FMNH<sub>2</sub>: red curves; FADH<sub>2</sub>: black curves).

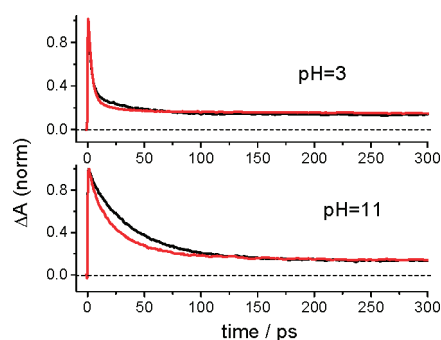


**Figure 5.** Upper panel: decay dynamics of transient signal at 500 nm obtained for pH = 5 solutions of FADH<sub>2</sub> (red curve) and FMNH<sub>2</sub> (black curve); lower panel: pH = 11 solution of FADH<sup>-</sup> (red curve) and FMNH<sup>-</sup> (black curve).

are essentially identical. This outcome shows that adenine has little effect on the excited-state properties of FADH<sup>-</sup>, which is consistent with the presence of the "open" conformer. A slight decrease in the excited-state lifetime of FADH<sup>-</sup> could be due to a certain degree of electron transfer to the adenine moiety. Due to the large distance between isoalloxazine and adenine in an "open" conformer, the rate for this electron transfer is probably too slow to significantly alter the spectroscopic signatures of the species involved.

The situation is different for FADH<sub>2</sub>. The absorption spectra of species involved in FADH<sub>2</sub> and FMNH<sub>2</sub> decay are different, as can be seen from Figure 4. The first two components of FADH<sub>2</sub> exhibit the same absorption spectra as those of FMNH<sub>2</sub>, and we assign them to two tautomers of FADH<sub>2</sub>. However, the longer-lived components ( $\tau_3$  and  $\tau_4$ ) exhibit completely different absorption spectra. We believe that those components arise from the radicals produced in two competing electron-transfer processes: (i) an intramolecular electron transfer from isoalloxazine to adenine and (ii) an electron transfer to the solvent to produce a solvated electron. Intramolecular electron transfer is expected to produce a flavin semiquinone radical with an absorption at  $\sim 510$  nm<sup>37</sup> and an adenine radical anion which absorbs at 300 nm.<sup>40</sup> The spectrum of our continuum probe does not extend into the UV region, so we can detect only the absorption arising from semiquinone.

**TABLE 2: The Lifetimes for FMNH<sup>-</sup> and FADH<sup>-</sup> Excited State Decay in the Absence and Presence of TT-Dimer<sup>a</sup>**

	$\tau_1$ , ps	$\tau_2$ , ps	$\tau_3$
FMNH <sup>-</sup>	105	228	long
FMNH <sup>-</sup> and 3 mM TT-dimer	35	160	long
FADH <sup>-</sup>	71	175	long
FADH <sup>-</sup> and 3 mM TT-dimer	6	192	long

<sup>a</sup> The measurements were done in H<sub>2</sub>O/DMSO mixture.

It is interesting to note that the excited-state lifetimes of two flavin tautomers in FADH<sub>2</sub> are longer than those of FMNH<sub>2</sub> ( $\tau_1$  and  $\tau_2$  in Table 1). Intramolecular electron transfer in FADH<sub>2</sub> is expected to decrease the lifetime of flavin excited-state species. Thus, there must be another effect by which the adenine moiety modulates the flavin dynamics. Since we expect FADH<sub>2</sub> to be dominantly present in a “stacked” conformer, the close interaction between isoalloxazine and adenine could increase the “rigidity” of the isoalloxazine ring that would in turn decrease the rate of thermal deactivation of the excited state. The effect of this kind is commonly observed in flavoproteins containing reduced flavin chromophores,<sup>16</sup> where the excited-state lifetimes of reduced flavin are much longer than those of reduced flavin in solution due to increased rigidity of the protein environment. Thus, the adenine moiety increases the flavin excited-state lifetimes by increasing the rigidity of the isoalloxazine moiety, while it decreases the excited-state lifetime by facilitating an intramolecular electron transfer process. The overall effect is a slight increase in the values for  $\tau_1$  and  $\tau_2$ .

**TT-Dimer Repair via FMNH<sup>-</sup> and FADH<sup>-</sup>.** We further investigated the repair dynamics of TT-dimer by flavins. These experiments were conducted at pH = 8, where the flavin exists in a deprotonated form ( $pK_a = 6.7^{31}$ ). We chose to study deprotonated flavin because (i) this is the flavin form that exists in DNA photolyase<sup>3</sup> and (ii) it was previously found that the deprotonation of flavin is required for the TT-dimer repair to occur.<sup>41</sup> Because of the low water solubility of TT-dimer, the experiments were conducted in H<sub>2</sub>O/DMSO solvent mixture. The excited-state decays of FMNH<sup>-</sup> and FADH<sup>-</sup> in H<sub>2</sub>O/DMSO mixture (Table 2) show a trend similar to those obtained in H<sub>2</sub>O (Table 1). A decrease in FADH<sup>-</sup> lifetimes relative to those of FMNH<sup>-</sup> is attributed to an intramolecular electron transfer process from the isoalloxazine to the adenine moiety of FADH<sup>-</sup>.

An interesting effect is observed in the TT-dimer repair studies. Lower panels of Figure 6 compare excited-state decays of FADH<sup>-</sup> and FMNH<sup>-</sup> cofactors at varying concentrations of TT-dimer. The flavin excited-state decays faster with an increasing TT-dimer concentration due to the repair process. However, the decrease in lifetime is much more pronounced in the case of FADH<sup>-</sup> ( $\tau_1$  in Table 2). The decay curves were fit to three-exponential decay functions. Because of the complexity of the excited-state behavior of reduced flavins, it is difficult to assign unambiguously the decays to specific transient species. In FMNH<sup>-</sup> and FADH<sup>-</sup> samples with no TT-dimer present, we assign  $\tau_1$  and  $\tau_2$  decays to two bent conformers of isoalloxazine moiety (see previous section). In the presence of TT-dimer, it is very likely that the decay with lifetime  $\tau_1$  originates from one of the flavin conformers. The decrease in the value of  $\tau_1$  is consistent with a photoinduced electron transfer to the TT-dimer. However, the decay with lifetime  $\tau_2$  could originate either from the second conformer of flavin or from the decay of a flavin semiquinone radical due to electron recombination from the “repaired” thymine radical anion to the semiquinone. Since  $\tau_2$  of FADH<sup>-</sup> increases in the presence of TT-dimer, we assign this decay to the semiquinone radical. This

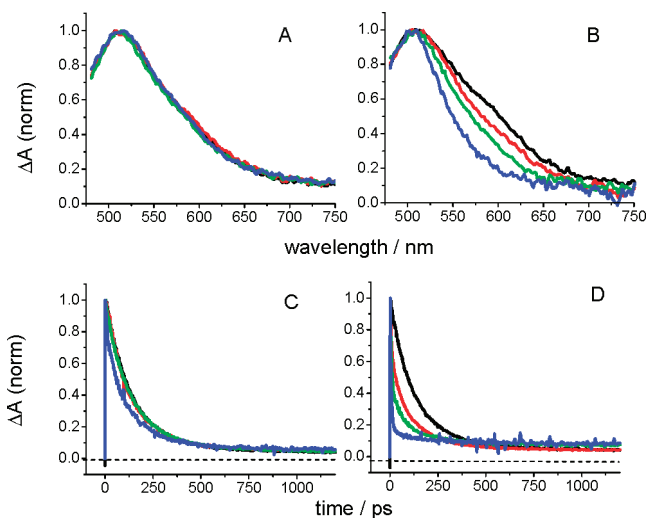
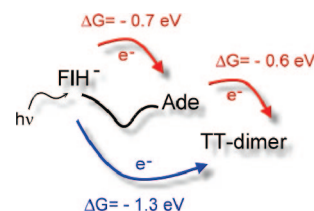


**Figure 6.** Transient absorption spectra (A and B) and decays (C and D) of FMNH<sup>-</sup> (left panels A and C) and FADH<sup>-</sup> (right panels B and D) in the presence of varying concentration of TT-dimer: 0 mM (black), 1 mM (red), 2 mM (green), and 3 mM (blue). The spectra were obtained 3 ps after the excitation pulse. The decays were obtained at  $\lambda = 515$  nm.

#### SCHEME 6: Two Possible Repair Mechanisms for TT-Dimer Repair via FADH<sup>-</sup> Cofactor<sup>a</sup>



<sup>a</sup> The standard reduction potential for TT-dimer used in  $\Delta G$  calculation is  $E = -1.9$  V.<sup>43</sup>

assignment is also supported by the spectral changes observed 3 ps after the excitation pulse (upper panels of Figure 6). While FMNH<sup>-</sup> samples show no change in the excited-state absorption spectra with increased TT-dimer concentration, FADH<sup>-</sup> spectra exhibit a successive blue-shift of the absorption maximum with increased TT-dimer concentration. This blue-shift is consistent with the formation of a semiquinone radical (absorption maximum 495 nm) and has also been observed in FADH<sub>2</sub> sample ( $\tau_3$  and  $\tau_4$  components in Figure 4).

Faster TT-dimer repair observed in FADH<sup>-</sup> could suggest that the adenine moiety of FADH<sup>-</sup> contributes to the TT-dimer repair efficiency by facilitating a two-step electron transfer mechanism (Scheme 6). Let us consider how the dynamics at 515 nm would be influenced by this two-step mechanism. The decay at 515 nm contains contributions from two species: the flavin excited-state and the semiquinone radical. In FMNH<sup>-</sup>, the flavin excited-state decays because of direct electron transfer from flavin excited-state to TT-dimer, while in FADH<sup>-</sup> the decay is a competition between electron transfer to adenine and electron transfer to TT-dimer. Electron transfer to adenine is already given by a decay of FADH<sup>-</sup> in the absence of TT-dimer. Thus, if the repair occurs via a two-step mechanism, the flavin excited states of FMNH<sup>-</sup> and FADH<sup>-</sup> should have different lifetimes in the absence of TT-dimer but should show the same decrease in the excited-state lifetime as the concentration of TT-dimer is increased. While we indeed observe different lifetimes in the absence of TT-dimer, we also observe different decay dynamics in the presence of TT-dimer. According to a

two-step electron-transfer model, these differences cannot be assigned to the flavin excited state. Let us now consider how the signal arising from semiquinone would be altered by a two-step mechanism. In FMNH<sup>-</sup>, semiquinone lifetime is determined by the rate of electron recombination from the thymine radical anion (T<sup>•-</sup>). In FADH<sup>-</sup>, semiquinone lifetime is determined by three recombination processes: (i) from the adenine radical anion, (ii) from T<sup>•-</sup> produced in a direct repair process, and (iii) from T<sup>-</sup> produced in a two-step repair process. Thus, it is possible that the FADH<sup>-</sup> dynamics observed at 515 nm arise from faster semiquinone recombination dynamics due to a two-step mechanism. As we described in the previous section, FADH<sup>-</sup> adopts an "open" conformer in which the rate of electron transfer between isoalloxazine and adenine is small. Thus, if the adenine moiety mediated the TT-dimer repair dynamics, its effect would be observed on the longer time scale. This is not consistent with our experimental results where differences in dynamics occur only few ps after the excitation pulse. Thus, faster TT-dimer repair by FADH<sup>-</sup> most probably does not originate from a two-step repair process. Because of high complexity of the excited-state dynamics of reduced flavins and a large overlap in the absorption spectra of the species involved in the repair, it is impossible to fully rule out this mechanism.

Another explanation can be offered for faster TT-dimer repair by FADH<sup>-</sup>. It arises from an interesting observation that the quenching process occurs at surprisingly low concentrations of TT-dimer. At 3 mM concentration of TT-dimer, the average distance between flavin and TT-dimer is too high (~100 Å) for molecules to diffuse toward each other within the excited-state lifetime (diffusion length ~10 Å). Thus, it appears that the TT-dimer concentrates around the flavins because of hydrophobic interactions. In light of this argument, it is possible that the increased quenching in FADH<sup>-</sup> arises because of the hydrophobic nature of adenine that attracts TT-dimer molecules.

## Conclusions

The excited-state dynamics of several flavin cofactors in the reduced form were studied using femtosecond optical transient absorption spectroscopy. FMNH<sup>-</sup> exhibits multiexponential decay dynamics, which were assigned to the presence of two bend conformers of the isoalloxazine ring ( $\tau_2$  and  $\tau_3$  in Table 1). In addition to the decay from two conformers, FMNH<sup>-</sup> also exhibits a long-lived component ( $\tau_4$ ) that was assigned to absorption from the semiquinone radical and the hydrated electron. In the case of FMNH<sub>2</sub>, an additional short-lived decay component ( $\tau_1$ ) was observed and assigned to the presence of an iminol tautomer. Adenine containing cofactors exhibit an additional complexity in their excited-state dynamics that arises because of intramolecular electron transfer from the isoalloxazine to the adenine moiety of the molecule. This effect is more pronounced in FADH<sub>2</sub>, where the two moieties are in close proximity to each other.

We also compared the efficiency of TT-dimer repair using FMNH<sup>-</sup> and FADH<sup>-</sup>. We find a faster repair using FADH<sup>-</sup>. One possible explanation for this behavior is a two-step electron-transfer mediated by the adenine moiety of FADH<sup>-</sup>. However, it is not likely that this mechanism explains the faster repair dynamics observed in our data. It is more probable that the efficient TT-dimer repair via FADH<sup>-</sup> arises from the fact that FADH<sup>-</sup> preferentially solvates TT-dimer molecules. FMNH<sup>-</sup>

is less hydrophobic than FADH<sup>-</sup> and thus does not offer as good environment for TT-dimer molecules.

**Acknowledgment.** This project is partly supported by ACS PRF (46807-G4). The measurements were conducted at the Ohio Laboratory for Kinetic Spectrometry. We thank Michael J. Rodgers and Eugene Danilov for their help with the laser measurements.

## References and Notes

- Briggs, W. R.; Christie, J. M. *Trends Plant Sci.* **2002**, 7 (5), 204–210.
- Gomelsky, M.; Klug, G. *Trends Biochem. Sci.* **2002**, 27 (10), 497–500.
- Sancar, A. *Chem. Rev.* **2003**, 103 (6), 2203–2237.
- Cashmore, A. R. *Cell* **2003**, 114 (5), 537–543.
- Kao, Y.-T.; et al. *Proc. Natl. Acad. Sci. U.S.A.* **2005**, 102 (45), 16128–16132.
- Sancar, G. B.; et al. *J. Biol. Chem.* **1987**, 262 (1), 478–85.
- Antony, J.; Medvedev, D. M.; Stuchebrukhov, A. A. *J. Am. Chem. Soc.* **2000**, 122 (6), 1057–1065.
- Dym, O.; Eisenberg, D. *Protein Sci.* **2001**, 10 (9), 1712–1728.
- Barrio, J. R.; et al. *Proc. Natl. Acad. Sci. U.S.A.* **1973**, 70 (3), 941–943.
- Heelis, P. F. *Chem. Soc. Rev.* **1982**, 11 (1), 15–39.
- Kondo, M.; et al. *J. Phys. Chem. B* **2006**, 110 (41), 20107–20110.
- Chosrowjan, H.; et al. *Chem. Phys. Lett.* **2003**, 378 (3–4), 354–358.
- Stanley, R. J.; MacFarlane, A. W. I. V. *J. Phys. Chem. A* **2000**, 104 (30), 6899–6906.
- van den Berg, P. A. W. *J. Phys. Chem. B* **2002**, 106 (34), 8858–8869.
- Li, G.; Glusac, K. D. *J. Phys. Chem. A* **2008**, 112 (20), 4573–4583.
- Leenders, R.; et al. *Eur. J. Biochem.* **1993**, 211 (1–2), 37–45.
- Visser, A. *Eur. J. Biochem.* **1979**, 101 (1), 13–21.
- Ghisla, S.; et al. *Biochemistry* **1974**, 13 (3), 589–597.
- Enescu, M.; Lindqvist, L.; Soep, B. *Photochem. Photobiol.* **1998**, 68 (2), 150–156.
- Yalloway, G. N.; et al. *Biochemistry* **1999**, 38 (12), 3753–3762.
- Tauscher, L.; Ghisla, S.; Hemmerich, P. *Helv. Chim. Acta* **1973**, 56 (2), 630–643.
- Zheng, Y. J.; Ornstein, R. L. *J. Am. Chem. Soc.* **1996**, 118 (39), 9402–9408.
- Moonen, C. T. W.; Vervoort, J.; Muller, F. *Biochemistry* **1984**, 23 (21), 4868–4872.
- Moonen, C. T. W.; Vervoort, J.; Muller, F. *Biochemistry* **1984**, 23 (21), 4859–4867.
- Heelis, P. F.; Hartman, R. F.; Rose, S. D. *Photochem. Photobiol.* **1993**, 57 (6), 1053–1055.
- Jorns, M. S. *J. Am. Chem. Soc.* **1987**, 109 (10), 3133–3136.
- Wulff, D. L.; Fraenkel, G. *Biochim. Biophys. Acta* **1961**, 51, p. 332–9.
- Nikolaitchik, A. V.; Korth, O.; Rodgers, M. A. J. *J. Phys. Chem. A* **1999**, 103 (38), 7587–7596.
- Murakami, M.; Maeda, K.; Arai, T. *Chem. Phys. Lett.* **2002**, 362 (1–2), 123–129.
- Gampp, H.; et al. *Talanta* **1985**, 32, p. 95–101.
- Lowe, H. J.; Clark, W. M. *J. Biol. Chem.* **1956**, 221, 983–92.
- Kierkegaard, P. *Flavins Flavoproteins* **1971**, 1–22.
- Ghisla, S.; Massey, V. *Eur. J. Biochem.* **1989**, 181 (1), 1–17.
- Hall, L. H.; Bowers, M. L.; Durfor, C. N. *Biochemistry* **1987**, 26 (23), 7401–7409.
- Ireland J. F., P. A. H. W. *Adv. Phys. Org. Chem.* **1976**, 12, p. 131.
- Du, Y. K.; Price, E.; Bartels, D. M. *Chem. Phys. Lett.* **2007**, 438 (4–6), 234–237.
- Massey, V. *Biochem. Soc. Trans.* **2000**, 28, p. 283–296.
- Yamase, T. *Photochem. Photobiol.* **1981**, 34 (1), 111–114.
- Manoj, P.; et al. *Chem. Phys.* **2007**, 331 (2–3), 351–358.
- Shi, Y. M.; et al. *Biochim. Biophys. Acta* **2000**, 1474 (3), 383–389.
- Hartman, R. F.; Rose, S. D. *J. Am. Chem. Soc.* **1992**, 114 (9), 3559–3560.
- Farhataziz, M. J. R. *Radiation Chemistry*; VCH Publishers: New York, 1987336.
- Heelis, P. F.; et al. *Int. J. Radiat. Biol.* **1992**, 62 (2), 137–43.